



## COMPUTATIONAL FLUID DYNAMICS ANALYSIS OF DIFFERENT GEOMETRIES FOR A JET STIRRED REACTOR FOR FUEL RESEARCH

**Leandro Alves de Oliveira, leandroalves@labcet.ufsc.br**

**Amir R. De Toni, detoni@labcet.ufsc.br**

**Leonel R. Cancino, leonel@labcet.ufsc.br**

**Amir A. M. Oliveira, amir.oliveira@ufsc.br**

Combustion and Thermal Systems Engineering Laboratory – LabCET

Department of Mechanical Engineering

Federal University of Santa Catarina

Brazil

**Edimilson Oliveira, edimil@petrobras.com.br**

**Mauro Iurk Rocha, miurk@petrobras.com.br**

PETROBRAS/CENPES/PDAB/COMB

Av. Horácio Macedo, 950

Cidade Universitária - Ilha do Fundão

21941-598 - Rio de Janeiro – RJ

Brazil

**Abstract.** *This work presents an analysis of different geometries for jet stirred reactor (JSR) employing computational fluid dynamics (CFD). The JSR is widely used in combustion studies due to its ability to promote rapid mixing and spatial homogeneity. Several geometrical configurations have been proposed in order to achieve homogeneous mixtures, but the extent of mixing may vary considerably among the possible designs, specially when one considers the large variation of fuels and operation conditions that may be found in the applications. An extensive literature review resulted in the development of an initial geometry and a series of simulations were performed to evaluate geometric modifications. The aim of this step-by-step analysis is to obtain a reactor geometry yielding homogeneous temperature, species and pressure, while allowing for easy manufacturing. A series of full multicomponent, turbulent, compressible, steady state numerical simulations were performed in Fluent® 14.0 with kerosene ( $C_{12}H_{23}$ ) and air (21%  $O_2$ , 79%  $N_2$ ) at stoichiometric composition. The JSR operation pressure and temperature were fixed at 4 bar and 900 K respectively.*

**Keywords:** *Jet stirred reactor, Fuel research, Computational fluid dynamics*

### 1. INTRODUCTION

Nowadays, control and modeling of combustion process are necessary to aid the design of combustion devices in order to obtain high efficiency, low emissions and fuel quality based on its kinetic aspects. As a result, significant increment in detailed kinetics data has been published over the last years.

Several chemical kinetics mechanisms at wide range of physical conditions covering distinct applications have been developed and proposed for mixtures and pure fuels (Cancino et al., 2013). The validation of these kinetic models requires experimental data and in order to obtain it, different experimental techniques have been used: flames supported by burners, static reactors, plug-flow reactors, shock tubes and continuous-flow stirred reactors (Dagaut et al., 1986).

The jet stirred reactor (JSR) is a continuous-flow stirred reactor and an important experimental tool in kinetic studies because it allows accurate monitoring of the extent of reaction by residence time control and its theory is focused on chemical kinetics phenomena (Longwell and Weiss, 1955; Matras and Villiermaux, 1965). In this experiment, operation and modeling features are strongly related with fluid dynamics: species transport, velocity, pressure, temperature, and turbulence profiles. In the literature, some realizations of this reactor were proposed and employed, but computational fluid dynamics (CFD) analysis of this kind of device are scarce (Gil and Mocek, 2012).

The present work is part of an ongoing research project aiming at the development and testing of alternative fuel mixtures, including biofuels. Additional information, including the use of detailed chemical kinetics simulations to predict the JSR capabilities, is reported in other articles by the same authors in these proceedings.

## 2. FUNDAMENTALS

### 2.1 Perfectly stirred reactor and jet stirred reactor

The perfectly stirred (PSR), or well stirred (WSR), reactor is an ideal reactor widely used in combustion and chemical engineering studies. Its modeling assumes instantaneous and homogeneous mixing of reactants and products, and constant temperature and pressure profiles inside the reactor. Furthermore, the steady state operation means no time dependence, and the equations describing the reactor are a set of coupled nonlinear algebraic equations. This simple reaction system has been used to several kinetics studies and to obtain values for global reaction parameters (Turns, 2012).

The jet stirred reactor (JSR) is an important experiment, it is approach of behavior of ideal perfectly stirred reactor, employing jets to increase stirring by jets interaction, swirl flow and more turbulence. It usually operates with high dilution level (about 100-1000 ppm of fuel) to achieve low gradients of transported properties inside the reactor, focusing only on chemical kinetics. The heat transfer problem and turbulence aspects are very important, and compressible effects in injectors must be evaluated.

### 2.2 Proposed geometries

Several geometries for PSR and JSR were proposed in the literature. Spherical, cylindrical (Clarke et al., 1958) and toroidal (Nenniger et al., 1984) configurations were developed in combustion studies. In this work, a spherical geometry was selected because it favors mixedness and uniformity of heat transfer and species transport. Spherical reactors described in the literature: Longwell and Weiss (1955), Clarke et al. (1958); Hottel and Schneider (1965); Kidd (1965); Jenkins and Yumlu (1967); David and Matras (1973); Osgerby (1973); Dagaut et al (1986); Lignola and Reverchon (1986); Cavaliere and Ciajolo (1993); and Joannon et al. (2005).

The first analyzed geometry Figure 1a, similar to the one studied by Kidd (1965), is simple and employs radial jets to perform mixing but presented far from ideal mixing and homogeneous temperature in the rear region of jets. The second configuration Figure 1b, uses a disc to distribute the reactants radially and presents low turbulence in radial inlet jet, creating non-uniformity on species profile. The third geometric proposal Figure 1c is more complex and it has several holes in a hemispherical premixing region arranged to generate turbulence and jets interaction but the results were not significantly improved. This configuration was proposed as a variation of the Longwell reactor (Longwell and Weiss, 1955). The fourth geometry Figure 1d has four injectors located in the hemispherical premixing region to improve jets mixing. This kind of configuration was conceived by Matras and Villermaux (1973) and it has been employed by Dagaut et al. (1986), Lignola and Reverchon (1986), Cavaliere and Ciajolo (1993), Joannon et al. (2005), and Herbinet et al. (2007). This geometry shown better results and it was selected to geometrical enhancement. Various geometries were proposed and evaluated but more results are omitted for brevity.

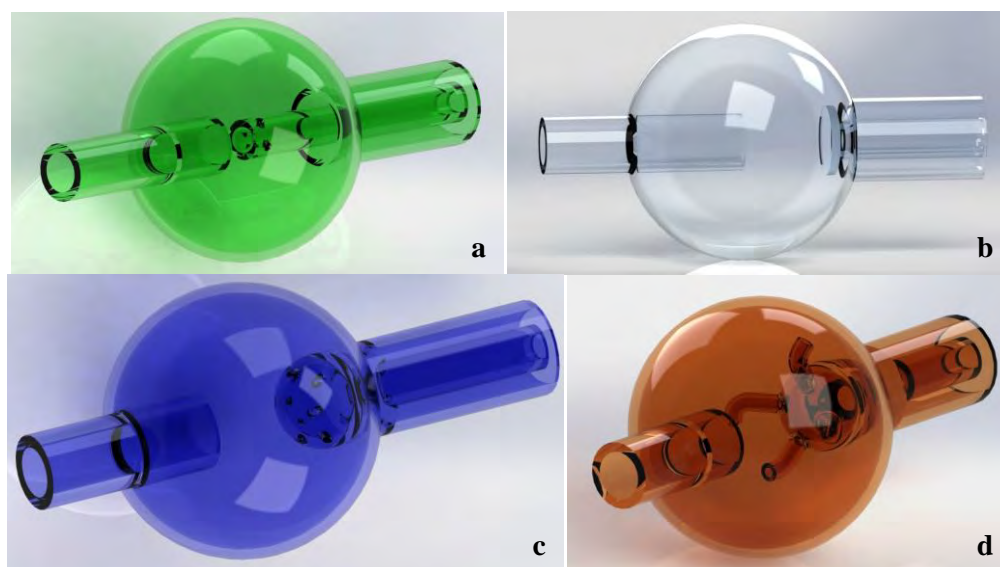


Figure 1. Proposed and evaluated geometries of JSR

After the numerical assessment of all the proposed geometries, by using CFD, a geometrical improvement was performed to the fourth geometry, adopting the guidelines of Matras and Villermaux (1973) and CFD analysis. This methodology resulted at an enhanced geometry configuration shown in Figure 2.

This enhanced geometry has a hemispherical premixing region fed by two concentric inlet pipes: the outer for  $O_2/N_2$  mixture and the inner for  $C_{12}H_{23}/N_2$  mixture. The mixture then flows through the four injectors with nozzles Figure 2, filling the reactor with a swirled, high turbulent flow, spreading the reactants homogeneously. The outlet pipe is also close to the equatorial plane of the spherical reactor, in order to generate better residence time distribution.

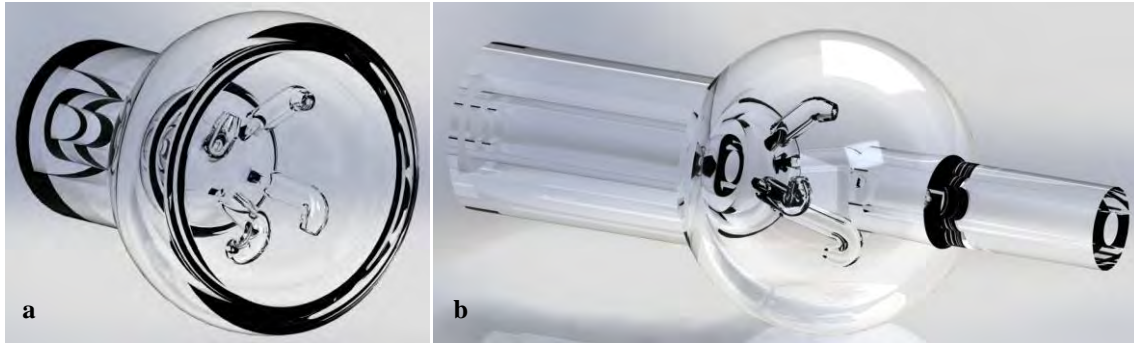


Figure 2. Enhanced geometry of the jet stirred reactor

### 2.3 Evaluated parameters

The improvement process was conducted to achieve a compromise between theoretical and attainable conditions. Thus, the main parameters evaluated in the simulations were species, temperature, pressure and turbulent intensity profiles in this order. Other additional parameter analyzed was the pressure loss, as an important parameter in experiment design and operation.

The expected results should exhibit low gradients of species, homogeneous temperature and pressure profiles inside the reactor, as well as high Mach number (about 0.8) and turbulence intensity in the injector's nozzles.

## 3. FLUID DYNAMICS ANALYSIS

### 3.1 Computational domain and mesh

The computational domain comprises the following regions of the enhanced geometry: two concentric inlet pipes, four injectors, hemispherical premixing zone, spherical reactor and outlet pipe, Figure 3a. The boundaries include four surfaces:  $O_2/N_2$  mixture inlet,  $C_{12}H_{23}/N_2$  mixture inlet, reactor's walls and outlet. Some geometrical simplifications were done in the edge's interfaces to improve the mesh quality (equiangular skewness) without significant differences from the real geometry.

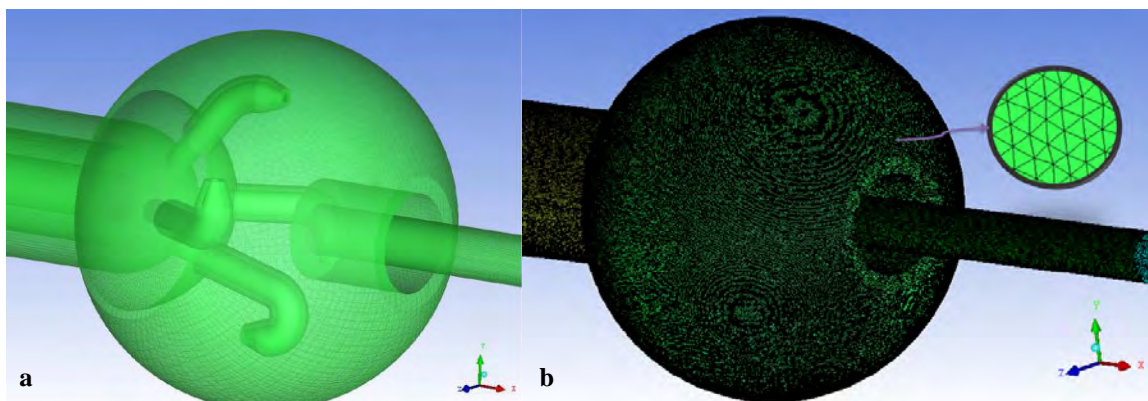


Figure 3. Computational domain and mesh

In the numerical assessment of the improved geometry, three unstructured meshes were used. The software ICEM CFD 14.0 was employed as mesh generator. The first mesh has 7.3 million volumes with quality between 0.54-0.95. The second mesh has 14.1 million volumes with quality between 0.50-0.95 and it was refined on regions with crucial gradients, like at the nozzles, hemispherical premixing region, and reactor's wall. The third and final mesh has 24.7 million volumes with quality between 0.50-0.95, Figure 3b. Table 1 shows the overall characteristics of meshes and their quality.

### 3.2 Numerical Model

The numerical simulations were performed assuming steady-state, three dimensional, compressible and turbulent flow, with species transport without chemical reaction. The boundary conditions prescribe inlet flow of mixture (kerosene and air).

Table 1. Mesh characteristics.

Mesh properties	Mesh 1	Mesh 2	Mesh 3
Number of volumes	7.3 million	14.1 million	24.7 million
Number of nodes	1.3 million	2.4 million	4.3 million
Maximum volume, m <sup>3</sup>	6.93e-11	4.258e-11	1.58e-11
Minimum volume, m <sup>3</sup>	6.41e-14	1.402e-14	5.83e-15
Minimum quality	0.542	0.501	0.505
Maximum quality	0.950	0.949	0.952

The Fluent® 14.0 software employs finite-volume methods to numerically solve the discrete, coupled differential conservation equations of mass, energy, momentum and species transport. For three dimensional, compressible, turbulent, steady-state problem, the set of conservation equations can be formulated as:

for mass balance

$$\nabla \cdot (\rho \vec{V}) = 0 \quad (1)$$

where  $\rho$  is density and  $\vec{V}$  is the velocity, for momentum balance

$$\nabla \cdot (\rho \vec{V} \times \vec{V}) = \nabla \cdot \vec{\sigma}_{eff} - \nabla p \quad (2)$$

where  $\vec{\sigma}_{eff}$  is the effective stress on fluid and  $p$  is the pressure, for energy balance

$$\nabla \cdot (h \vec{V}) = \nabla \cdot [k_{eff} \nabla T] + \mu \Phi + S^\phi \quad (3)$$

where  $h$  is the enthalpy,  $k_{eff}$  is the effective thermal conductivity,  $T$  is the temperature,  $S^\phi$  allows all the source terms, and  $\mu \Phi$  are the viscid terms of energy equation.

The selected material was a mixture of kerosene and air from Fluent® 14.0 database. The considered compounds were kerosene (C<sub>12</sub>H<sub>23</sub> as surrogate for kerosene), molecular oxygen (O<sub>2</sub>) and molecular nitrogen (N<sub>2</sub>).

Species transport without chemical reaction was selected for a mixture of kerosene and air, and then two equations for transported species must be resolved for kerosene and molecular oxygen, while molecular nitrogen computed by balance. Thermal and full multicomponent diffusion were implemented with coefficients calculated internally in Fluent® 14.0 by using kinetic theory. The simulations do not included fuel oxidation since the study is focused on fluid dynamic response of the proposed geometries. The steady-state species transport equation can be formulated as

$$\nabla \cdot (\rho \vec{V} \phi_i) = 0 \quad (4)$$

where  $\phi_i$  is the concentration of the “ $i$ ” chemical specie.

Two-equation models are complete and can be used to predict properties of a given turbulent flow with no prior knowledge of the turbulence structure (Wilcox, 1993). For comparative purposes, the  $k$ - $\epsilon$  and  $k$ - $\omega$  turbulence models (two-equation models) were used, due to their ability to evaluate different turbulent flow aspects with relatively reduced computational cost. These models compute the transport of the turbulent kinetic energy,  $k$ , and also the turbulent length scale or equivalent.

The first model selected was standard  $k$ - $\varepsilon$ , the most popular two-equation model of turbulence. Its actual closure coefficients and form was referred to Launder and Sharma (1974). The basic idea is to derive the exact equation for dissipation rate,  $\varepsilon$ , and to find suitable closure approximations. Several terms in the expression are experimental because they are essentially impossible to measure with any degree of accuracy. The experimental closure coefficients transform the model in an approximation and are used to parameterize various terms in the modeled  $\varepsilon$  equation as functions of large-eddy scales (Wilcox, 1993). The standard  $k$ - $\varepsilon$  is described by the following equations:

$$\rho \frac{\partial k}{\partial t} + \rho V_j \frac{\partial k}{\partial x_j} = \tau_{ij} \frac{\partial V_i}{\partial x_j} - \rho \varepsilon + \frac{\partial}{\partial x_j} \left[ \left( \frac{\mu + \mu_T}{\sigma_k} \right) \frac{\partial k}{\partial x_j} \right] \quad (5)$$

$$\rho \frac{\partial \varepsilon}{\partial t} + \rho V_j \frac{\partial \varepsilon}{\partial x_j} = C_{\varepsilon 1} \frac{\varepsilon}{k} \tau_{ij} \frac{\partial V_i}{\partial x_j} - C_{\varepsilon 2} \rho \frac{\varepsilon^2}{k} + \frac{\partial}{\partial x_j} \left[ \left( \frac{\mu + \mu_T}{\sigma_\varepsilon} \right) \frac{\partial \varepsilon}{\partial x_j} \right] \quad (6)$$

$$\mu_T = \frac{\rho C_\mu k^2}{\varepsilon} \quad (7)$$

where  $\mu$  is the viscosity,  $V_i$  is the component "i" of velocity vector,  $x_j$  is a "j" dimension,  $\tau_{ij}$  is a shear stresses on fluid,  $C_{\varepsilon 1}$ ,  $C_{\varepsilon 2}$ ,  $\sigma_\varepsilon$ ,  $\sigma_k$ ,  $C_\mu$  are the standard empirical coefficients, and  $\mu_T$  is the eddy viscosity (Wilcox, 1993).

The second turbulence model used in this work was standard  $k$ - $\omega$ , the first two-equation model proposed by Kolmogorov (1942). The more extensively tested  $k$ - $\omega$  model and with standard closure coefficients approximation is referred to Wilcox (1988). This model adds a second parameter, the specific dissipation rate,  $\omega$ , to describe the turbulent transport of properties. The standard  $k$ - $\omega$  is described by the following equations:

$$\rho \frac{\partial \kappa}{\partial t} + \rho V_j \frac{\partial \kappa}{\partial x_j} = \tau_{ij} \frac{\partial V_i}{\partial x_j} - \beta^* \rho \kappa \omega + \frac{\partial}{\partial x_j} \left[ (\mu + \sigma^* \mu_T) \frac{\partial \kappa}{\partial x_j} \right] \quad (8)$$

$$\rho \frac{\partial \omega}{\partial t} + \rho V_j \frac{\partial \omega}{\partial x_j} = \alpha \frac{\omega}{\kappa} \tau_{ij} \frac{\partial V_i}{\partial x_j} - \beta \rho \omega^2 + \frac{\partial}{\partial x_j} \left[ (\mu + \sigma \mu_T) \frac{\partial \omega}{\partial x_j} \right] \quad (9)$$

$$\mu_T = \frac{\rho \kappa}{\omega} \quad (10)$$

Where  $\alpha$ ,  $\beta$ ,  $\beta^*$ ,  $\sigma$ ,  $\sigma^*$  are the standard empirical coefficients, and  $\mu_T$  is the eddy viscosity (Wilcox, 1993).

The boundary conditions are shown on Tab. 2. Stoichiometric composition was employed and mass-flow values were obtained by simulation of chemical kinetic mechanisms for chemical surrogates of kerosene in CHEMKIN-PRO software, considering 80% of fuel conversion (De Toni et al., 2013; Cancino et al., 2013). The temperature condition was tuned to achieve around 900 K inside reactor, and to avoid significant  $\text{NO}_x$  formation.

The numerical simulation is essentially unstable due to the presence of several complex features (phenomenology) such as compressible flow, high-turbulence, complex and with high curvature geometry, high gradients of transported properties in the nozzles and pre-mixed region. Thus, convergence control by under relaxation was necessary to achieve numerical stability. Table 3 show under relaxation factors applied as defined by authors. The SIMPLE method for pressure-velocity coupling was selected, including second order schemes to calculate properties. The second order schemes were selected to better describe the phenomena and high gradients.

Table 2. Boundary conditions parameters

Parameter	Value
Mass-flow inlet (O <sub>2</sub> /N <sub>2</sub> )	Mass-flow = 1.4053 g/s. Temperature = 1100 K. Turbulence model = hydraulic diameter and turbulent intensity (8%). Mass fraction: [O <sub>2</sub> ]= 0.3057; [N <sub>2</sub> ]=0.6943.
Mass-flow inlet (C <sub>12</sub> H <sub>23</sub> /N <sub>2</sub> )	Mass-flow = 0.5647 g/s. Temperature: 300 K. Turbulence model: hydraulic diameter and turbulent intensity (5%). Mass fraction: [C <sub>12</sub> H <sub>23</sub> ] = 0.2237; [N <sub>2</sub> ] = 0.7763.
Walls	No slip condition, constant roughness (0.5). Not heat transfer. No species deposition.
Outlet	Operating as outlet pressure. Turbulence model: hydraulic diameter and turbulent intensity (8%).

Table 3. Under relaxation factors ( $k$ - $\epsilon$ ) and ( $k$ - $\omega$ )

Pressure, $p$	0.2	Dissipation rate, $\epsilon$ Specific dissipation Rate, $\omega$	0.7
Density, $\rho$	0.8	Concentration of kerosene, [C <sub>12</sub> H <sub>23</sub> ]	0.8
Momentum, $V$	0.6	Concentration of oxygen, [O <sub>2</sub> ]	0.8
Turbulent kinetic energy, $k$	0.7	Energy, $h$	0.8

## 4. RESULTS

### 4.1 Fluid Dynamics Results

A series of full multicomponent, -transport species, -turbulent, compressible, steady state numerical simulations were performed in Fluent® 14.0 with kerosene (C<sub>12</sub>H<sub>23</sub>) and air (21% O<sub>2</sub>, 79% N<sub>2</sub>) at stoichiometric composition. This methodology has been executed for two geometries: initial geometry Figures 4-7 and enhanced geometry Figures 8-11; and for two turbulence models:  $k$ - $\epsilon$  Figures 4-5 and 8-9, and  $k$ - $\omega$  Figures. 6-7 and 10-11.

The presented results are profiles of kerosene concentration, Mach number, temperature and turbulent intensity. These properties have been selected to discuss the results and to qualitatively evaluate the geometrical improvement since they are closely related to the main characteristics of the reactor:

- The kerosene concentration profile was selected to evaluate the mixing process and homogeneity of species;
- Mach number, to show compressible effects and velocity aspects;
- Temperature, to exhibit its homogeneity as well as heat transfer, diffusion and mixing phenomena;
- Turbulent intensity to evaluate the influence of turbulence.

Two different planes, that better represent global profiles inside the reactor, are used as the baseline for the data-post-processing, to show fluid-dynamics features. In this work, only the results of the non-enhanced geometry are presented and discussed since numerical models setup are analogous and mesh properties were very similar.

The computational resources employed in simulation processes were two workstations Dell Precision T7500 with 48 GB of RAM and 6 Intel Xeon Processors. The finer mesh simulations demanded around 250 hours and 350 hours of computation respectively.

### 4.2 Discussion

The numerical results of Figures 4-11 are reasonable for both geometries but some differences may defy aspects of the improvement process. An important aspect is good agreement of numerical results to both turbulence models. The more crucial aspects about property profiles can be synthesized as:

- The concentration of kerosene contours for all numerical models were very similar. The maximum spatial variation was about  $5 \times 10^{-3}$  and the average value was near and around  $6.4 \times 10^{-2}$  that corresponds to the global stoichiometric value. The initial geometry presents a larger region with non-uniformity species concentration in front of injector's outlet, as a result of lower turbulent intensity while the injector with nozzle improves the turbulent effects at enhanced geometry. This effect is intensified in numerical model employing  $k$ - $\omega$  turbulence model.

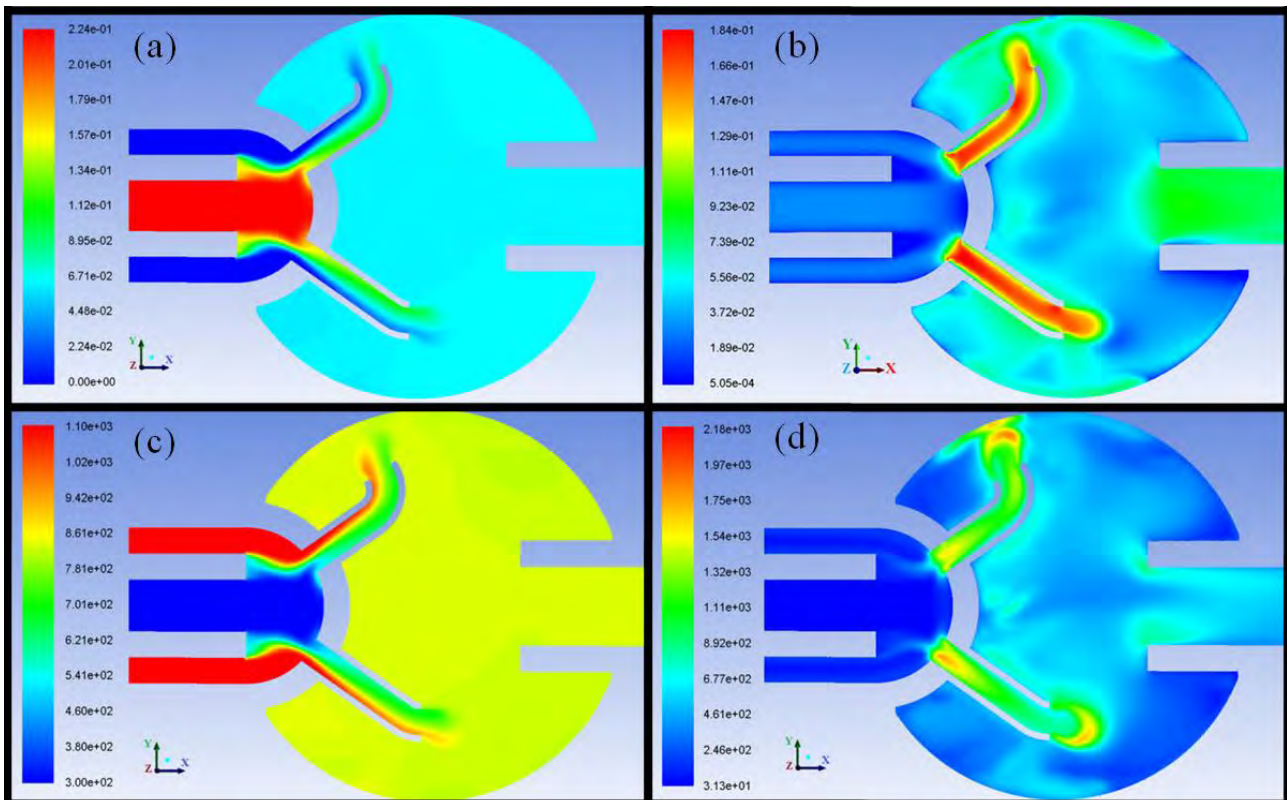


Figure 4. Results of initial geometry for plane z ( $k-\epsilon$  model):  
a. Concentration of kerosene, [-]; b. Mach number, [-]; c. Static temperature, [K]; d. Turbulent intensity [ $m^2/s^2$ ].

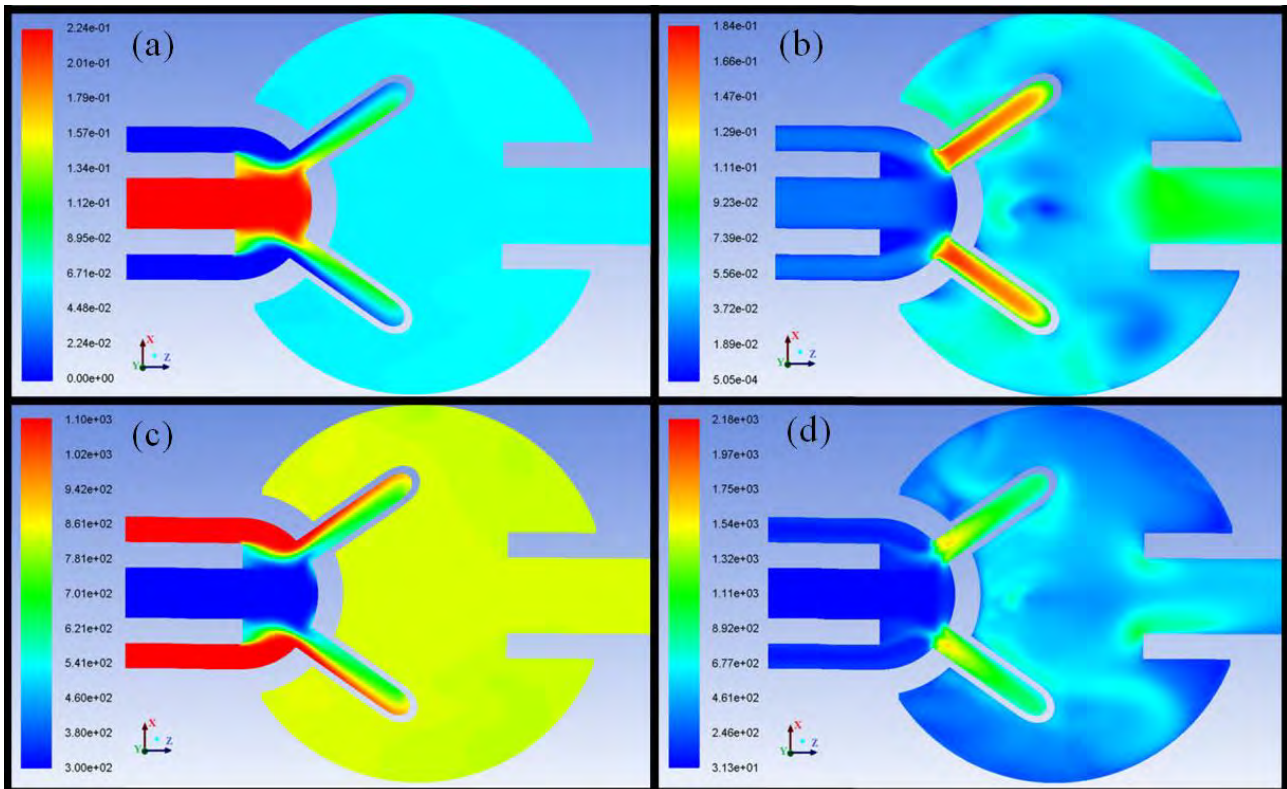


Figure 5. Results of initial geometry for plane y ( $k-\epsilon$  model):  
a. Concentration of kerosene, [-]; b. Mach number, [-]; c. Static temperature, [K]; d. Turbulent intensity [ $m^2/s^2$ ].

OLIVEIRA, L.A., DE TONI, A.R.; CANCINO, L.R., ROCHA, I.M., OLIVEIRA, E. and OLIVEIRA, A.A.M.  
 A Jet Stirred Reactor Geometry: A Computational Fluid Dynamics Analysis

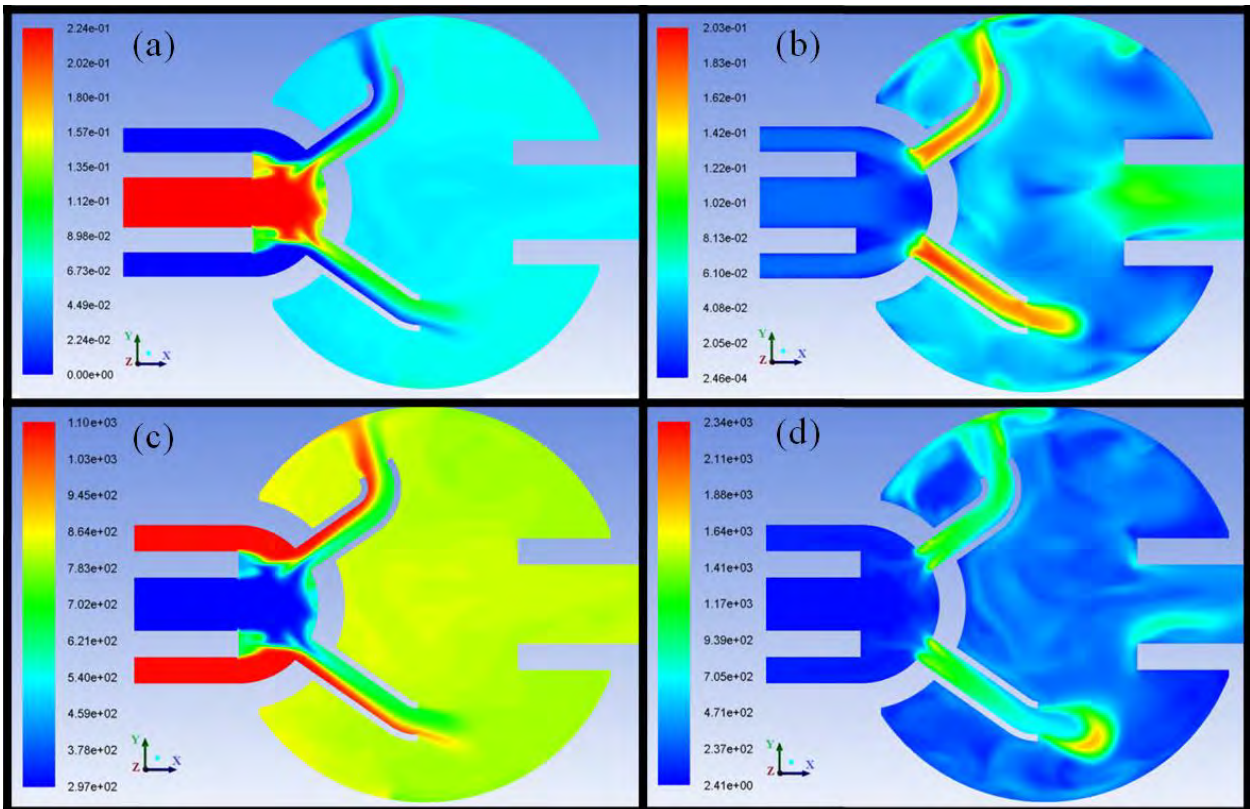


Figure 6. Results of initial geometry for plane z (k- $\omega$  model):  
 a. Concentration of kerosene, [-]; b. Mach number, [-]; c. Static temperature, [K]; d. Turbulent intensity [ $m^2/s^2$ ].

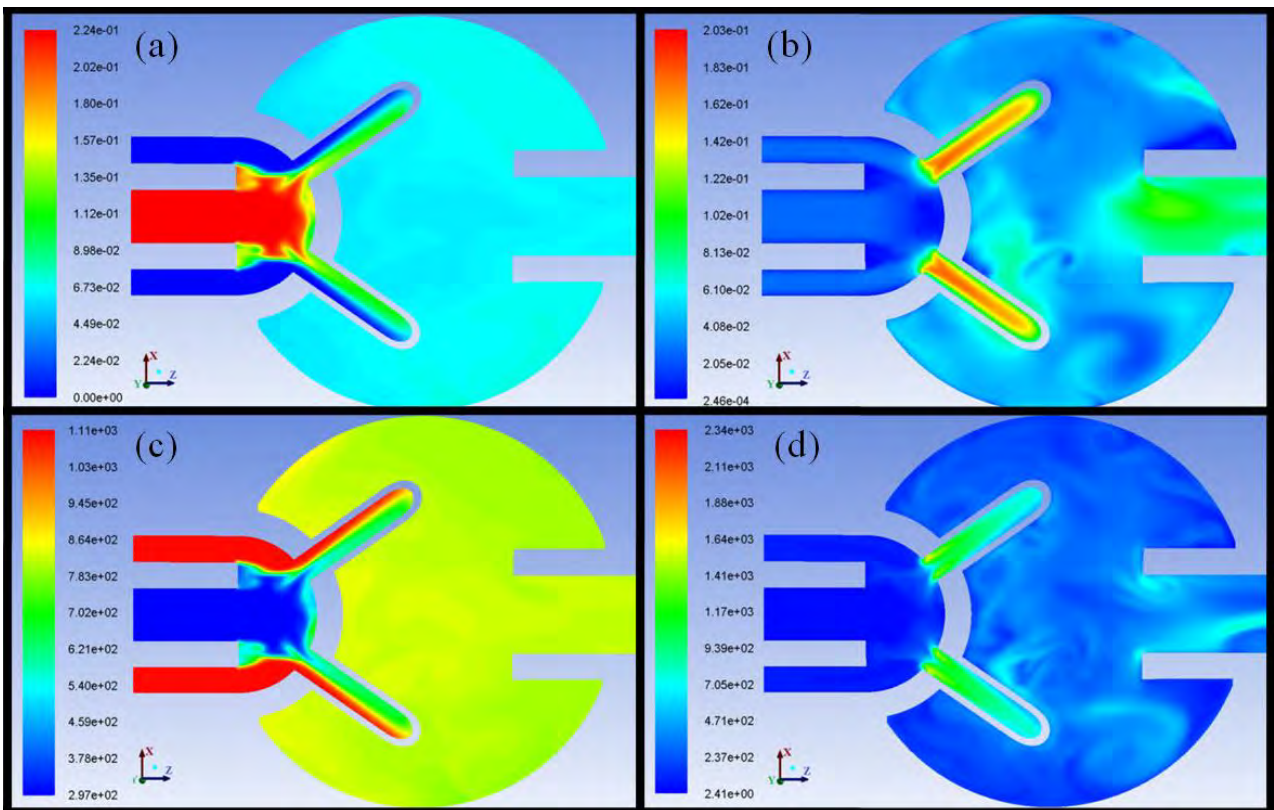


Figure 7. Results of initial geometry for plane y (k- $\omega$  model):  
 a. Concentration of kerosene, [-]; b. Mach number, [-]; c. Static temperature, [K]; d. Turbulent intensity [ $m^2/s^2$ ].

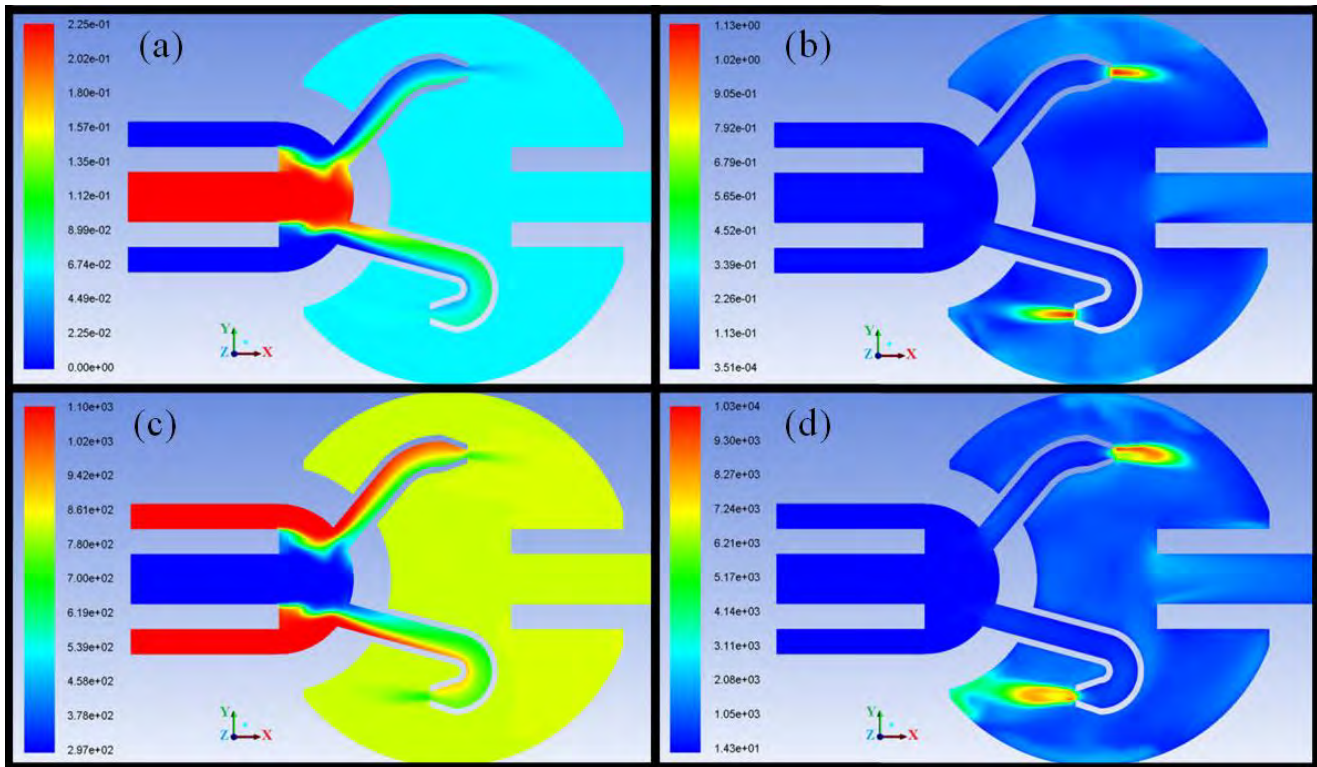


Figure 8. Results of improved geometry for plane z (k-ε model):  
a. Concentration of kerosene, [-]; b. Mach number, [-]; c. Static temperature, [K]; d. Turbulent intensity [ $\text{m}^2/\text{s}^2$ ].

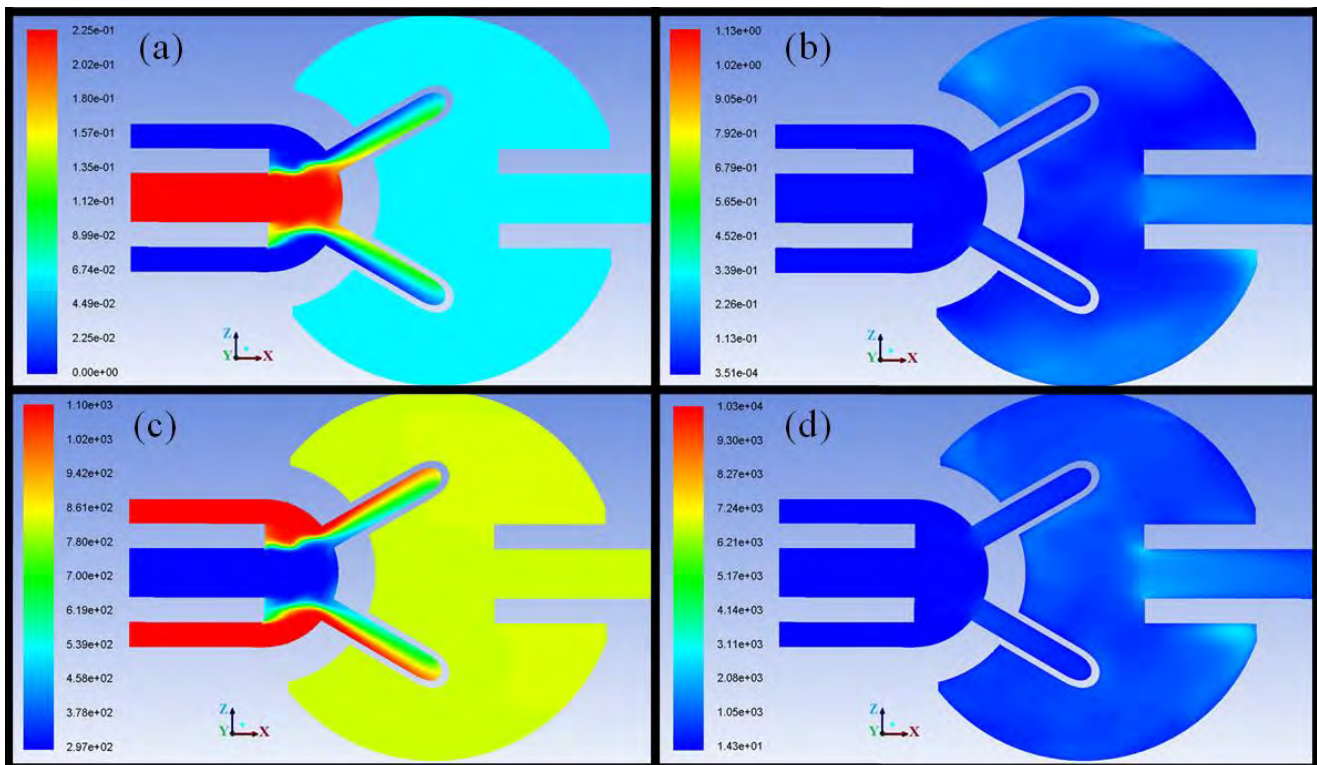


Figure 9. Results of improved geometry for plane y (k-ε model):  
a. Concentration of kerosene, [-]; b. Mach number, [-]; c. Static temperature, [K]; d. Turbulent intensity [ $\text{m}^2/\text{s}^2$ ].

OLIVEIRA, L.A., DE TONI, A.R.; CANCINO, L.R., ROCHA, I.M., OLIVEIRA, E. and OLIVEIRA, A.A.M.  
 A Jet Stirred Reactor Geometry: A Computational Fluid Dynamics Analysis

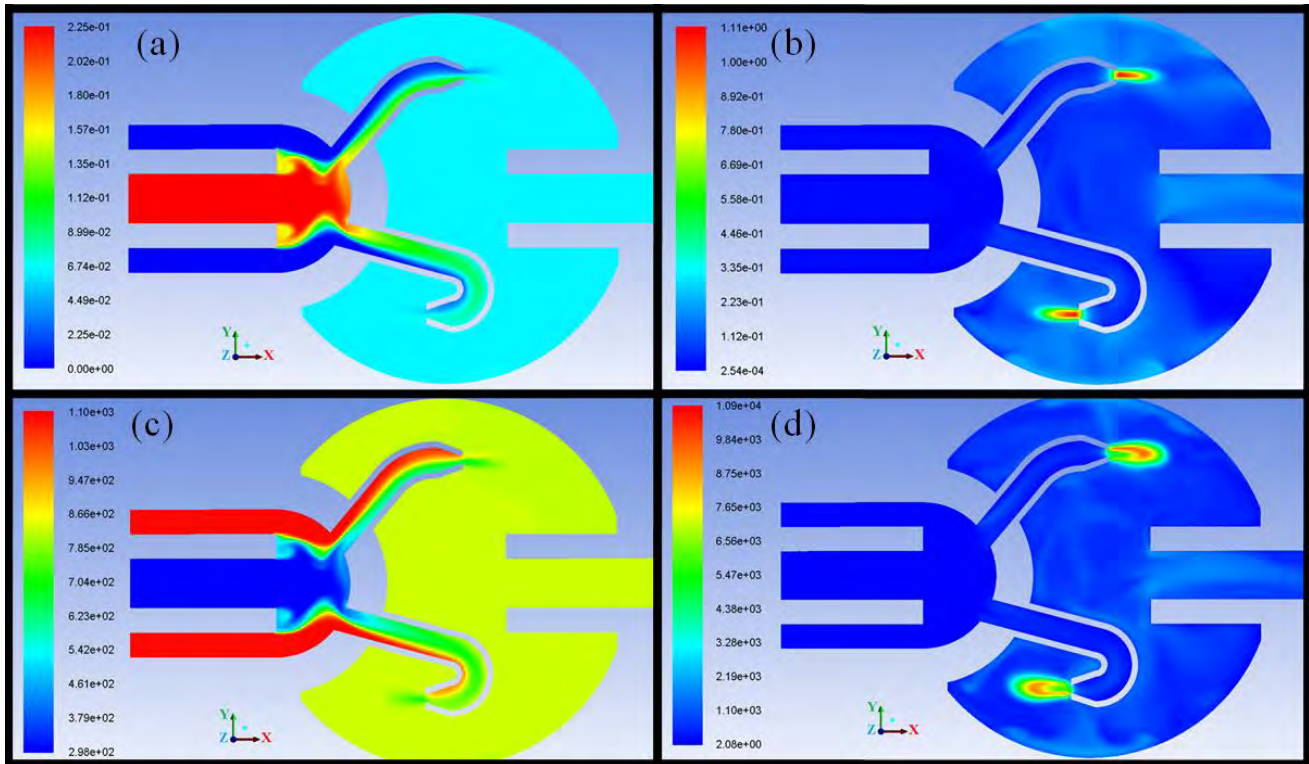


Figure 10. Results of improved geometry for plane z (k- $\omega$  model):  
 a. Concentration of kerosene, [-]; b. Mach number, [-]; c. Static temperature, [K]; d. Turbulent intensity [ $m^2/s^2$ ].

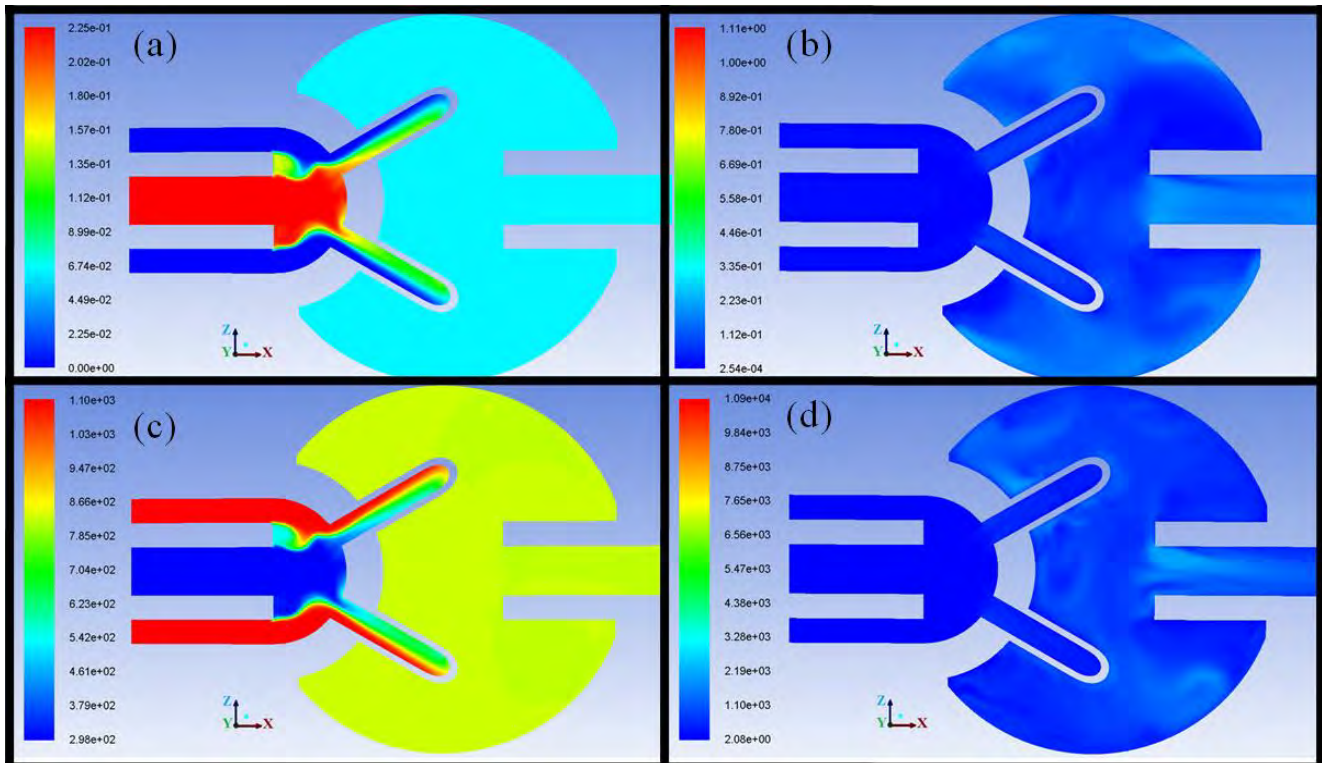


Figure 11. Results of improved geometry for plane y (k- $\omega$  model):  
 a. Concentration of kerosene, [-]; b. Mach number, [-]; c. Static temperature, [K]; d. Turbulent intensity [ $m^2/s^2$ ].

- The Mach number profiles present similarity with turbulent intensity profiles. The initial geometry did not present compressible effects, with a maximum Mach number around 0.18 ( $k-\epsilon$ ) and 0.20 ( $k-\omega$ ), but the enhanced geometry presents important compressible effects, with a maximum Mach number of 1.14. This results in high pressure loss and operation troubles;
- The temperature profiles for all models were very similar too. Its maximum spatial variation inside spherical reactor in all results is about 40 K (considering jets zone) and the average value is around 860 K. The improved geometry presents better homogeneity in temperature profile due to more turbulence.
- The turbulent intensity profiles show increase of turbulence, mainly in the jets. This results in better mixing process and homogeneous temperature field. However, generates compressible effects that affect pressure profile and pressure loss.

The pressure profiles, not present here, were approximately uniform for all cases. The improved geometry presents higher pressure gradient and pressure loss, caused by increment of compressible and turbulent effects, and of velocity. The pressure loss was about 5.4 atm in the improved geometry.

## 5. CONCLUSIONS

Therefore, by analysis of results the improved geometry related of initial geometry shows better mixing process, increment of turbulence, and more homogeneity on temperature profile, but compressible effects and more spatial variation of pressure were generated. Other important aspect, it is the effect on chemical kinetics phenomena in the region with high Mach number, which it was a bad result and corrections in nozzle diameter are necessary.

How the reactor operates with high dilution level and the effect of temperature is more representative than pressure in chemical kinetics, the enhanced geometry improve the two main theoretical characteristics of JSR: mixing and homogeneous temperature profile.

## 6. ACKNOWLEDGEMENTS

The authors acknowledge the financial support of PETROBRAS.

## 7. REFERENCES

- BLINCHNER, O.; 1961. "A fluid dynamic study of a spherical and a cylindrical stirred reactor", *Eighth symposium (international) on combustion*, volume 8, issue 1, pp 995-1002.
- CAVALIERE, A.; CIAJOLO, A.; D'ANNA, A.; MERCOGLIANO, R.; RAGUCCI, R.; 1993. "Autoignition of n-heptane and n-tetradecane in engine-like conditions", *Combustion & flame*, volume 93, issue 3, pp.279-286.
- CANCINO, L.R.; ROCHA, I.M.; OLIVEIRA, E.; OLIVEIRA, A.A.M.; 2013. "Isocetane (C<sub>16</sub>H<sub>34</sub>), hexadecane (C<sub>16</sub>H<sub>34</sub>) and Methyl-Cyclohexane (C<sub>7</sub>H<sub>14</sub>) as fuel surrogates: a numerical study of the ignition delay time", COBEM 2013.
- CLARKE, A. E., HARRISON, A. J.; ODGERS, J.; 1958. "Combustion stability in a spherical combustor", *Symposium (international) on combustion*, volume 7, issue, pp 664-673.
- CLARKE, A. E.; ODGERS, J.; RYAN, P.; 1961. "Further studies of combustion phenomena in a spherical combustor", *Eighth symposium (international) on combustion*, volume 8, issue 1, pp 982-994.
- CLARKE, A. E.; ODGERS, J.; STRINGER, F. W.; HARRISON, A. J.; 1965. "Combustion processes in a spherical combustor", *Tenth symposium (international) on combustion*, volume 10, issue 1, pp 1151-1166.
- DAGAUT, P., CATHONNET, M., ROUAN J.P., FOULATIER, R., QUILGARS, A., BOETTNER, J. C., GAILLARD, F., JAMES, H., 1986. "A jet-stirred reactor for kinetic studies of homogeneous gas-phases reactions at pressures up to ten atmospheres (~1 MPa)", *J. Phys. E: Sci. Instrum.*, vol 19, pp. 207-209.
- ENGLEMAN, V. S.; BARTOK, W.; LONGWELL, J. P.; 1973. "Experimental and theoretical studies of NO<sub>x</sub> formation in a jet-stirred combustor", *Fourteenth symposium (international) on combustion*, volume 14, issue 1, pp 755-765.
- DE TONI, A.R., OLIVEIRA, L.A.; CANCINO, L.R.; ROCHA, I.M.; OLIVEIRA, E.; OLIVEIRA, A.A.M.; "Perfectly stirred reactor: numerical assessment of gaseous fuels combustion for reactor dimensioning", COBEM 2013.
- FERRER, M.; DAVID, R.; VILLERMAUX, J; 1984. "Homogeneous oxidation of n-butane in a self-stirred reactor", *Chemical engineering and processing: process intensification*, volume 19, issue 3, pp 119-127.
- FLUENT 6.3, 2006; "User's guide", Lebanon NH: Fluent Inc.
- GIL, I.; MOCEK, P.; 2012. "CFD analysis of mixing intensity in jet stirred reactors", *Chemical and Process engineering*, volume 3, issue 3, pp 397-410.
- GLARBORG, P.; MILLER, J. A.; KEE, R. J.; 1986. "Kinetic modeling and sensitivity analysis of nitrogen oxide formation in well-stirred reactors", *Combustion & flame*, volume 65, issue, pp 177-202.
- HAWTHORNE, W. R.; WEDDELL, D. S.; HOTTEL, H. C.; 1949. "Mixing and combustion in turbulent gas jets", *Third symposium on combustion and flame, and explosion phenomena*, volume 3, Issue 1, pages 266-288.

OLIVEIRA, L.A., DE TONI, A.R.; CANCINO, L.R., ROCHA, I.M., OLIVEIRA, E. and OLIVEIRA, A.A.M.  
A Jet Stirred Reactor Geometry: A Computational Fluid Dynamics Analysis

- HERBINET, O.; MARQUAIRE, P.M.; BATTIN-LECLERC, F.; FOURNET, R.; 2007. "Thermal decomposition of n-dodecane: experiments and kinetic modeling", *Journal of analytical and applied pyrolysis*, volume 78, issue 2, pages 419-429.
- HOTTEL, H. C.; WILLIAMS, G. C.; BAKER, M. L.; 1957. "Combustion studies in a stirred reactor", *Sixth international symposium on combustion*, volume 6, Issue 1, pp 398-411.
- HOTTEL, H. C.; WILLIAMS, G. C.; BONNELL, A. H.; 1958. "Application of well-stirred reactor theory to the prediction of combustor performance", *Combustion & flame*, volume 2, issue 1, pp 13-34, 1958.
- HOTTEL, H. C.; WILLIAMS, G. C.; 1965. "Kinetic studies in stirred reactors: combustion of carbon monoxide and propane", *Tenth symposium (international) on combustion*, volume 10, issue 1, pp 111-121.
- HOTTEL, H. C., WILLIAMS, G. C., MILES, G. A., "Mixedness in well stirred reactor", *Tenth symposium (international) on combustion*, volume 11, issue 1, pp 771-778.
- JENKINS, D. R., YUMLU, V. S.; 1967. "Combustion of hydrogen and oxygen in a steady-flow adiabatic stirred reactor", *International Symposium on Combustion*, Volume 11, Issue 1, pp 779-790, 1967.
- JOANNON, M de; CAVALIERE, A.; FARAVELLI, T.; RANZI, E.; SABIA, P.; TREGROSSI, A.; 2005. "Analysis of process parameters for steady operation in methane mild combustion technology", *Proceedings of the combustion institute*, volume 30, issue 2, pages 2605-2612.
- LIGNOLA, P. G., REVERCHON, E., 1986. "Dynamics of n-heptane and i-octane combustion processes in a jet stirred flow reactor operated under pressure", *Combustion & flame*, volume 64, issue 2, pp 177-183, Napoly, Italy, 1986.
- LONGWELL, J.P.; WEISS, M.A.; 1955. "High Temperature Reaction Rates in Hydrocarbon Combustion", *Ind. Eng. Chem.*, 47 (8), pp 1634-1643.
- KIDD, P. H.; FOSS, W. I.; 1965. "Combustion of Fuel-lean mixtures in adiabatic well-stirred reactor", *Tenth symposium (international) on combustion*, volume 10, issue 1, pp 101-110.
- MATRAS, D.; VILLERMAUX, J.; 1973. "Un réacteur parfaitement agité par jets gazeux pour l'étude cinétique de réactions chimiques rapides", *Chem. Eng. Sci.*, volume 28, issue 1, pages 129-137.
- NENNIGER, J. E.; KRIDIOTIS, A.; CHOMIAK, J.; LONGWELL, J. P.; SAROFIM, A.F.; 1984. "Characterization of a toroidal well stirred reactor", *Twentieth symposium (internacional) on combustion*, pp 473-479.
- OSGERBY, I. T.; 1973. "Perfectly stirred reactor – new concept for a cw chemical laser", *Journal of applied physics*, volume 44, issue 1, pp 2627-2630.
- TURNNS, S.R.; 2012. "An Introduction to Combustion: Concepts and Applications", third edition, McGraw-Hill, United States, 565 p.
- WILCOX, D. C.; 1993. "Turbulence Modelling for CFD", First edition, DCW Industries, pp 460.
- WORMECK, J.J., PRATT, D. T., 1977. "Computer modelling of combustion in a longwell", *symposium (international)*, volume 16, issue 01, pp 1583-1592.

## 8. RESPONSIBILITY NOTICE

The authors are the only responsible for the printed material included in this paper.